# Chaotic state to self-organized critical state transition of serrated flow dynamics during brittle-to-ductile transition in metallic glass

C. Wang,[1] B. A. Sun,[2] W. H. Wang,[1] and H. Y. Bai[1,a)]
[1]*Institute of Physics, Chinese Academy of Sciences, Beijing 100190, China*
[2]*Centre for Advanced Structural Materials, Department of Mechanical and Biomedical Engineering, City University of Hong Kong, Kowloon Tong, Kowloon, Hong Kong*

(Received 1 December 2015; accepted 21 January 2016; published online 4 February 2016)

We study serrated flow dynamics during brittle-to-ductile transition induced by tuning the sample aspect ratio in a Zr-based metallic glass. The statistical analysis reveals that the serrated flow dynamics transforms from a chaotic state characterized by Gaussian-distribution serrations corresponding to stick-slip motion of randomly generated and uncorrelated single shear band and brittle behavior, into a self-organized critical state featured by intermittent scale-free distribution of shear avalanches corresponding to a collective motion of multiple shear bands and ductile behavior. The correlation found between serrated flow dynamics and plastic deformation might shed light on the plastic deformation dynamic and mechanism in metallic glasses. © *2016 AIP Publishing LLC*.
[http://dx.doi.org/10.1063/1.4941320]

## I. INTRODUCTION

Bulk metallic glasses (BMGs) present outstanding mechanical properties including large elastic limit and high strength.[1,2] These superior properties make BMGs important candidates as structural materials.[3] However, at temperatures far below the glass transition, the plastic deformation in BMGs is often characterized by shear localization where plastic strain is highly confined to one or a few narrow shear bands.[4,5] Because the propagation instability of the individual shear band finally leads to the catastrophic failure, resulting in limited plasticity in BMGs, great efforts have been made to improve the plasticity of BMGs through various methods.[6–10] For example, changing the sample aspect ratio can significantly improve the ductility of BMGs.[11–14] Due to the confinement of testing the crosshead of the machine during deformation, complex stress states induced by the friction between the crosshead and the specimen together with the mechanical interlocking inside the specimen, Zr-based specimens with an aspect ratio of 0.5 can be compressed into a flake without fracture.[11–14]

Owing to the disordered nature of glasses, the deformation mechanism of BMGs is completely different from the dislocation-mediated deformation in their crystalline counterparts. From a macroscopic viewpoint, mechanical behavior of BMGs such as plastic deformation is closely related to shear bands,[15] which, once initiated, often proceed in an intermittent manner and manifest as the serrated flow behavior in a stress-strain curve.[16,17] At the atomic scale, the plastic flow in BMGs is considered to comprise the local inelastic rearrangement of some defect-like clusters, often termed as flow units[18] and liquid-like zone.[19] Theories such as free volume[20] and shear transformation zone theory[21] are also proposed to explicate the atomic scale flow mechanism and to interpret the correlation between the macroscopic deformation behavior and microscopic structure heterogeneity.[22] Since the plastic flow of BMGs is an intrinsically dynamic process, the plastic deformation mechanism was recently discussed from the viewpoint of flow dynamics in BMGs. For example, it is found that the plastic deformation of ductile metallic glasses could evolve into a self-organized critical (SOC) state characterized by power-law distributed shear avalanches, which is closely related with multiple shear bands interaction during deformation.[15] Furthermore, the serrated flow is found to depend strongly not only on some external testing conditions such as strain rate and temperature but also on some internal conditions including elastic moduli and specimen geometry.[23,24] Therefore, the serrated flow can directly reflect the temporal behavior of shear banding and characterize the dynamic properties of shear bands during plastic deformation.

In this study, we attempt to understand the relationship between the plastic deformation mechanism and the serrated flow dynamics through their variation during a brittle-to-ductile transition induced by the changing sample aspect-ratio of a typical $Zr_{64.13}Cu_{15.75}Ni_{10.12}Al_{10}$ BMG. By performing a series of compression tests with different aspect ratios and serration statistical analyses for the BMG, we find a transition from chaotic dynamics to the SOC dynamics, which corresponds to the transition from the single shear band motion to the activation of multiple shear bands, macroscopically corresponding to the brittle-to-ductile transition. The plastic deformation mechanism in BMG is discussed in terms of the serrated flow dynamics behaviors.

## II. EXPERIMENTAL

Master alloy with a nominal composition of $Zr_{64.13}Cu_{15.75}Ni_{10.12}Al_{10}$ [in atomic present (at. %)] was prepared by arc melting pure elements under a Ti-gettered purified argon atmosphere. Homologous rod-shape samples with a diameter of 3 mm were prepared by suction casting a master alloy ingot into a water-cooled copper mold. The details of

a)Author to whom correspondence should be addressed. Electronic mail: hybai@aphy.iphy.ac.cn

 

the preparation of the BMG are referred to in Ref. 13. The glassy nature was verified by X-ray diffraction (XRD) and differential scanning calorimetry (DSC) with a heating rate of 20 K/min. The samples for compression were cut from the same rod by the diamond saw with different aspect-ratios $A$ of 0.47, 0.56, 0.67, 0.73, 0.88, 0.91, 0.95, 0.99, 1.01, 1.03, 1.12, 1.35, and 1.80, respectively. The upper and bottom surfaces of the samples were carefully polished using a designed grinding apparatus to ensure parallelism. Compression tests were carried out on an Instron electromechanical 3384 test system at the strain rate of $2 \times 10^{-4}\,s^{-1}$ at room temperature with a data acquisition frequency of 30 Hz. After deformation, the fractography of the deformed samples was observed using a Hitachi S-4800 scanning electron microscope (SEM).

## III. RESULTS AND DISCUSSION

Figure 1 presents the typical true stress-strain curves of $Zr_{64.13}Cu_{15.75}Ni_{10.12}Al_{10}$ BMG with different aspect ratios, $A$. For samples with small aspect-ratios from 0.47 to 0.73, compression is stopped deliberately when plastic deformation approaches 40%–50%. It can be seen that the yielding strength gradually increases when the aspect ratio decreases in accordance with the previous observation of Wu *et al.*[25] Shown in the inset of Fig. 1, a brittle-to-ductile transition occurs when the aspect-ratio $A$ decreases: when the aspect-ratio approximates 2:1, the samples fail in a brittle manner without plastic deformation; while the aspect-ratio decreases, the plasticity gradually increases and finally the BMG sample can be compressed into a flake without catastrophic fracture. We note that the critical aspect-ratio for brittle-to-ductile transition is sensitive to the aspect-ratio, the strain rate, temperature, composition, and other testing conditions.[11,14] The critical aspect-ratio changes from 0.4 to 0.9 with a strain rate changing from $2 \times 10^{-1}\,s^{-1}$ to $10^{-6}\,s^{-1}$ (Ref. 14). To focus on the study of the serrated flow

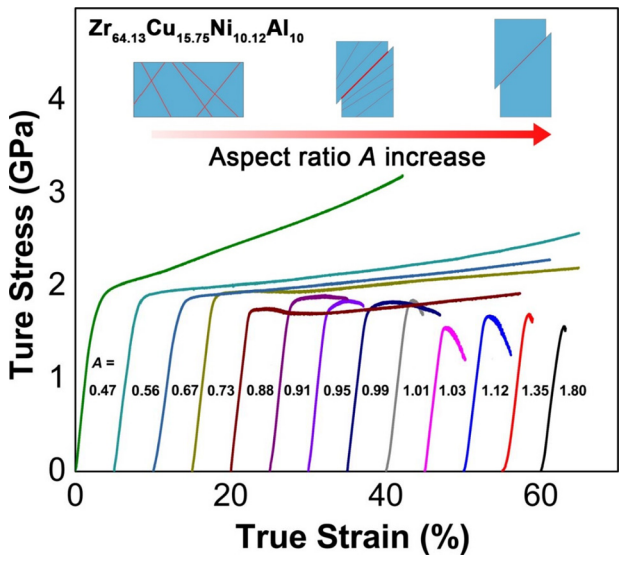


FIG. 1. True stress-strain curves (strain rate $= 2 \times 10^{-4}\,s^{-1}$) of $Zr_{64.13}Cu_{15.75}Ni_{10.12}Al_{10}$ with different aspect ratios. Inset is a schematic diagram of the brittle-to-ductile transition induced by decreasing aspect ratio.

dynamics during a brittle-to-ductile transition induced by changing the aspect-ratio, all our compression tests were carried out with the same strain rate of $2 \times 10^{-4}\ s^{-1}$ at room temperature.

All the samples with different aspect ratios exhibit serrated flow behavior as characterized by repeated cycles of a rapid stress drop followed by elastic reloading.[26] A close examination reveals that the serrated flow behavior changes with aspect ratio. As shown in Fig. 2(a), the serrations for ductile samples with aspect ratio $A = 0.73$ display multifarious sizes characterized by massive small serrations before a relatively larger serration, which are more complex than that of the brittle ones such as the one with $A = 1.03$. Meanwhile, the serration size for the ductile one is smaller than that of the brittle one. To systemically characterize the serrated flow behavior, we measured the magnitude of stress drops ($\Delta\sigma_s$) and then perform the statistical analysis on the data. Because the serrations in the initial stage of plastic deformation mainly originate from the formation of the shear band,[17] we only selected data of steady state serrated flow for statistics. Before the statistics, a normalization of subtracting the linear fitting from the elastic deformation region has to be done to rule out the influence of stress vibrations induced by the testing machine. As shown in Fig. 2(b), serrations with a stress drop magnitude less than 0.5 MPa are abandoned in the subsequent statistical analysis.[15] Meanwhile, as shown in Fig. 2(c), the stress drop magnitude gradually increases with time. This ascending trend of $\Delta\sigma_s$ versus time results from the slowly expanding of cross-sectional area, which is a geometric effect induced by sample barreling during compression and does not reflect the nature of shear band dynamics.[6,15] Through a linear fitting on stress drop magnitude versus time, $\overline{\Delta\sigma_s} = f(t)$, the baseline of $\Delta\sigma_s$ versus time is flattened out by $s = \frac{\Delta\sigma_s}{f(t)/f(t0)}$ [see Fig. 2(d)], where $f(t_0)$ is the fitted value at the starting time $t_0$ of statistics.[15] We note that both the stress drop and the elastic energy density stored in the serrated event can be the equivalent index for reflecting the serrated flow dynamics in glasses. The stress drop magnitude is in proportion to the shear bands displacement in a serrated event and the statistics of the stress drop magnitude can reflect the distribution of shear bands displacement, which is closely related to the mechanical behavior of the metallic glasses. To study the serrated flow dynamics during a mechanical behavior of brittle-to-ductile transition, we chose the stress drop to characterize the serrated flow behavior; thus, we can more directly reflect the origin of serrated flow induced by the mechanical behavior in these glasses.

Figure 3 exhibits the average normalized stress drop magnitude $\bar{s}$ as a function of $A$. It is evident that the $\bar{s}$ increases with increasing aspect ratio $A$. The burst of serrations is closely related to properties of the sample and testing conditions.[27,28] Based on the principle of energy balance and shear banding dynamics, the stress drop magnitude could be an indicator of the shear band stability.[29] In the perspective of single shear band dynamics,[23] the sample aspect-ratio influences the intrinsic dynamic instability of steady-state shear band sliding. As sample height decreases, the stress drop amplitude descends and finally disappears at a critical

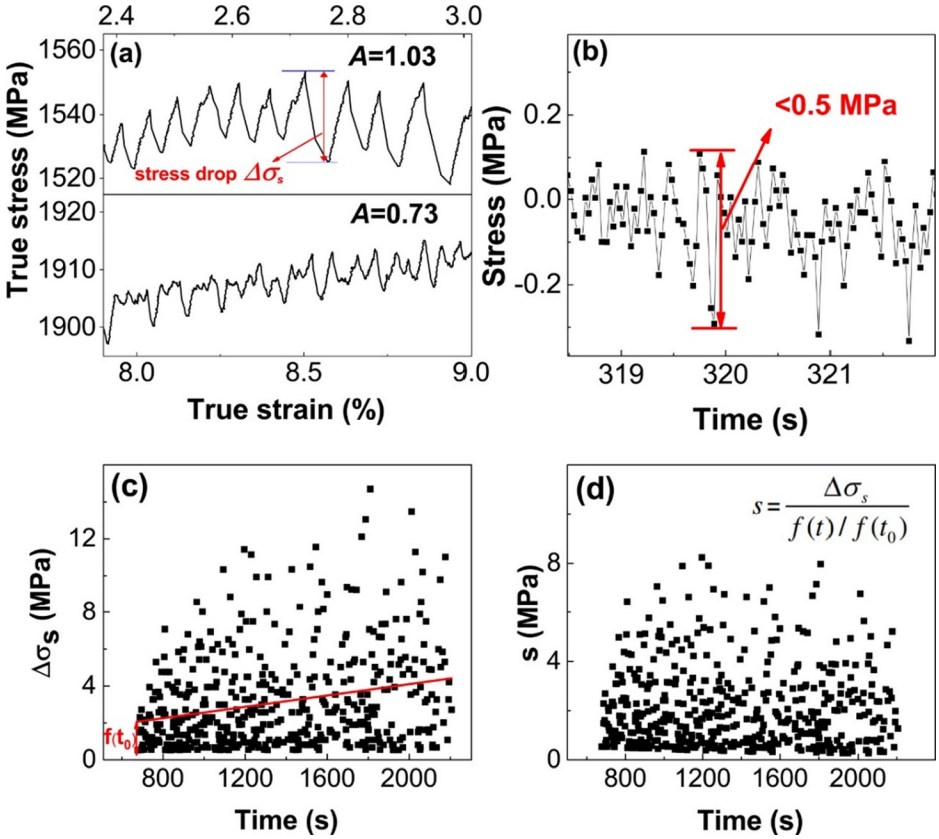


FIG. 2. (a) Comparison of serration behavior of samples with height of 3.10 mm and 2.00 mm, showing the stress drop of a serration. (b) Stress vibrations due to the environmental noise detected from the elastic region; stress drops less than 0.5 MPa are considered. (c) The curve of stress drop magnitude $\Delta\sigma_s$ versus time $t$, where the red line is the linear regression fit and the fitting value at the starting time $f(t_0)$ is labeled. (d) The curve of normalized stress drop magnitude $s$ versus time $t$.

height. After that, non-serrated flow dominates because shear banding tends to be more stable. In the case of multiple shear bands interaction, although serrated flow is more complex, the shear bands often follow the same critical instability conditions as the single shear band motion.[30] Therefore, with the same cross-sectional area, the smaller the sample aspect ratio, the more stable the shear banding.

The curve of mean stress drop magnitude versus aspect ratio $A$ could be divided into two parts. When the sample aspect-ratio is relatively larger (blue dashed line in Fig. 3), the changing rate of the $\bar{s}$ with the aspect ratio $A$ is larger than that with the smaller aspect-ratio (red dashed line in Fig. 3), and a transformation region between these two parts appears. The change in slope indicates the existence of plastic deformation mechanism transition as the sample aspect-ratio decreases. To characterize this phenomenon, the statistical analysis of stress drop magnitude is applied. Figure 4 shows the distribution histograms of normalized stress drop

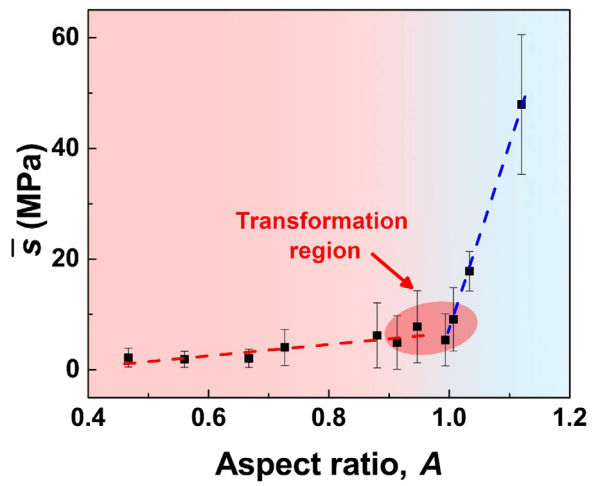


FIG. 3. Curve of mean normalized stress drop magnitude $\bar{s}$ as a function of aspect ratio $A$. The dashed lines in blue and red are the guide for the eyes.

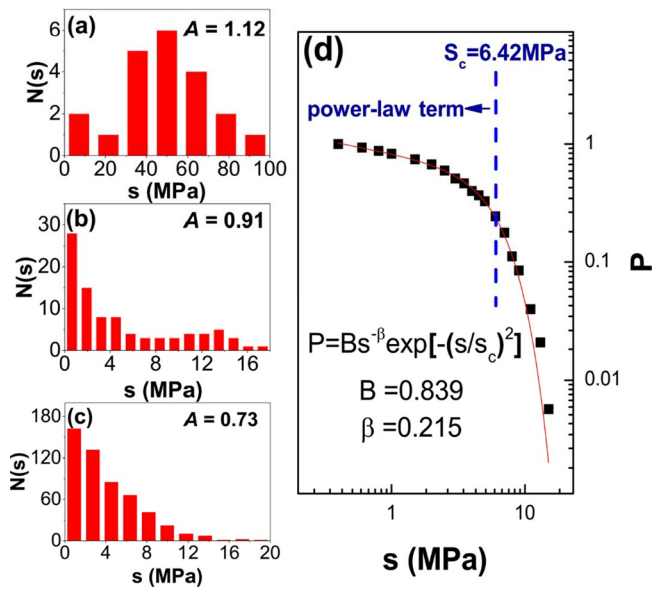


FIG. 4. The distribution histograms of statistical number $N(s)$ versus normalized stress drop magnitude s for samples with different aspect ratios of (a) 1.12, (b) 0.91, and (c) 0.73. (d) Logarithmic plot of the cumulative probability distribution $P$ of stress strops versus stress drop magnitude $s$ for the sample with aspect ratio of 0.73. Red line is the fitting curve of a power-law distribution with an exponential decay function.

magnitude $s$ for the samples with different aspect ratios, where $N(s)$ denotes the corresponding statistical number of $s$. The distribution histograms correlate closely with the aspect ratio as well as plasticity of the BMG. As shown in Fig. 4(a), for samples with the relative larger aspect ratio and plastic strain less than 5% (see in Fig. 1), most of the stress drop values fall in the range of 35–65 MPa and the distribution histogram displays a peak shape, which displays the feature of Gaussian-like distribution, indicating that the stress drop magnitude has a characteristic length scale, which often has a chaotic dynamic state by the time series analysis.[31] In crystalline materials, this kind distribution of stress drops is often termed as Portevin-Le Chatelier (PLC) effect, and the chaotic stick-slip originated from the pinning and reactivation of dislocations occurs.[32] In BMGs, the Gaussian-distributed serrated flow can be attributed to the stick-slip dynamics of single shear band, which reflects intrinsic dynamic instability of shear banding.[23]

In contrast to the serrations of the large aspect-ratio samples, as shown in Fig. 4(c), the distribution of stress drops for shorter samples with aspect ratio of 0.47, 0.56, 0.67, and 0.73, which can undergo large compression deformation (see in Fig. 1), is more complex and shows a decreasing trend. The percentage of stress drop magnitudes larger than a certain value, i.e., the cumulative probability distribution $P$, is calculated[33] and the calculated results are shown in Fig. 4(d). The curve of $P$ versus $s$ can be well fitted by a power-law distribution with an exponential decay function of

$$P = Bs^{-\beta}\exp[-(s/s_c)^2], \tag{1}$$

where $B$ is a normalized constant, $\beta$ is the scaling exponent with a fitting value of 0.215, and $s_c$ is the cut-off stress drop value fitted by 6.42 MPa, which characterizes the starting point of the exponential decay factor dominating. The fitting curve suggests that the distribution of stress drops for samples with small aspect ratio essentially follows a power-law distribution up to the critical value $s_c$, after that the exponential decay factor takes effect. The deviation at larger $s$ may arise from the size limited effect,[34] and the stress drop magnitude is only restrained by finite size of the system. The power-law distribution is often a signal of SOC phenomenon and suggests that the serration size is scale-free, which means that the microstructures at different length scales are similar. The SOC phenomenon implies that the system can buffer larger disturbance by dissipating external effect through cooperated motion of connected participants. In the case of BMGs, the relationship between SOC phenomenon with plasticity has been established,[15] and the occurrence of SOC implies the collective motion of multiple shear bands.

As shown in Fig. 4(b), when the aspect ratio is in the transformation region, the plasticity is partly enhanced, but the distribution histogram of stress drop magnitude is complex. As $A$ decreases, a transition trend from Gaussian distribution to power-law distribution in histogram occurs, which implies a transition in deformation mechanism occurs. It means that in the perspective of serrated flow dynamics, the shear band dynamics changes from chaotic state to self-organized critical state with sample aspect-ratio decreasing, implying that the deformation mechanism changes from single shear band stick-slip motion to collective motion of multiple shear bands. This change in deformation mechanism accounts for the observed brittle-to-ductile transition.

To directly probe shear band behavior, SEM photographs of side surfaces for samples with different aspect ratios are shown in Figs. 5(a)–5(c), which correspond to the distribution histograms in Figs. 4(a)–4(c), respectively. For the samples with very limited plasticity, only one dominant shear band is visible in Fig. 5(a), which corresponds to the stick-slip dynamics of single shear band characterized by Gaussian distributed stress drop magnitude. For the samples in the transformation region with enhanced plasticity shown in Fig. 5(b), the existence of some paralleled secondary shear

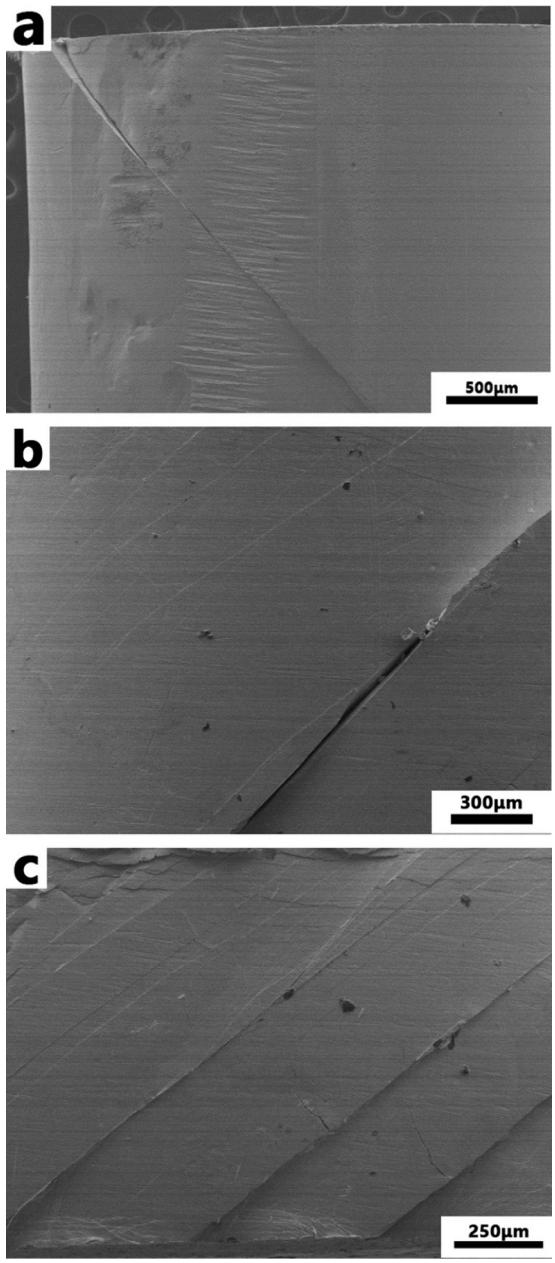


FIG. 5. SEM photographs of side surfaces for samples with aspect ratio of (a) 1.12, (b) 0.91, and (c) 0.73.

bands besides the dominate shear band hints the transition in the plastic deformation mechanism. As shown in Fig. 5(c), secondary shear bands, cracks between shear bands and massive shear bands paralleled to the surface due to friction between specimen and platen can be observed in the samples with small aspect-ratio, and these activated multiple shear bands lead to the stable large plasticity. The SEM photographs consist well with our statistical analysis of the serrated flow dynamics and the change of plastic deformation mechanism during the brittle-to-ductile.

## IV. CONCLUSION

In summary, our results show that, corresponding to a distinct brittle-to-ductile transition with the sample aspect ratio decreasing, the dynamics of serrated flow in the $Zr_{64.13}Cu_{15.75}Ni_{10.12}Al_{10}$ metallic glass transforms from a chaotic state characterized by Gaussian-like distributed serrations into a self-organized critical state featuring power-law distribution of shear avalanches. The transition of the dynamic serrated flow behavior indicates the plastic deformation mechanism changes from single shear band stick-slip motion to collective motion of multiple shear bands as aspect ratio decreases. The correlation found between the serrated flow dynamics and plasticity in BMG is helpful for the understanding the mechanism of plastic deformation in BMGs and may have implication for designing metallic glasses with large plasticity.

## ACKNOWLEDGMENTS

We thank D. Q. Zhao, D. W. Ding, B. B. Wang, Z. Wang, and Y. Z. Li for technical assistance and helpful discussions. The financial support of the NSF of China (Grant Nos. 51271195 and 5141101072) and the MOST 973 Program (No. 2015CB856800) are appreciated.

[1]W. H. Wang, Prog. Mater. Sci. **57**, 487 (2012).
[2]A. Inoue, B. Shen, H. Koshiba, H. Kato, and A. R. Yavari, Nat. Mater. **2**, 661 (2003).
[3]M. Ashby and A. Greer, Scr. Mater. **54**, 321 (2006).
[4]J. J. Lewandowski and A. L. Greer, Nat. Mater. **5**, 15 (2006).
[5]Y. Zhang and A. L. Greer, Appl. Phys. Lett. **89**, 071907 (2006).
[6]B. A. Sun and W. H. Wang, Prog. Mater. Sci. **74**, 211 (2015).
[7]C. C. Hays, C. P. Kim, and W. L. Johnson, Phys. Rev. Lett. **84**, 2901 (2000).
[8]Y. Wu, Y. Xiao, G. Chen, C. T. Liu, and Z. Lu, Adv. Mater. **22**, 2770 (2010).
[9]K. Yamano, Y. Yokoyama, K. Fukaura, and H. Sunada, Mater. Trans. **22**, 623 (2001).
[10]H. B. Yu, J. Hu, X. X. Xia, B. A. Sun, X. X. Li, W. H. Wang, and H. Y. Bai, Scr. Mater. **61**, 640 (2009).
[11]W. H. Jiang, G. J. Fan, H. Choo, and P. K. Liaw, Mater. Lett. **60**, 3537 (2006).
[12]Z. F. Zhang, H. Zhang, X. F. Pan, J. Das, and J. Eckert, Philos. Mag. Lett. **85**, 513 (2005).
[13]Y. H. Liu, G. Wang, R. J. Wang, Q. Zhao de, M. X. Pan, and W. H. Wang, Science **315**, 1385 (2007).
[14]H. Bei, S. Xie, and E. George, Phys. Rev. Lett. **96**, 105503 (2006).
[15]B. A. Sun, H. B. Yu, W. Jiao, H. Y. Bai, D. Q. Zhao, and W. H. Wang, Phys. Rev. Lett. **109**, 189904 (2010).
[16]R. B. Schwarz, W. J. Wright, and W. D. Nix, Mater. Sci. Eng., A **319–321**, 229 (2001).
[17]S. X. Song, H. Bei, J. Wadsworth, and T. G. Nieh, Intermetallics **16**, 813 (2008).
[18]Z. Lu, W. Jiao, W. H. Wang, and H. Y. Bai, Phys. Rev. Lett. **113**, 045501 (2014).
[19]J. C. Ye, J. Lu, C. T. Liu, Q. Wang, and Y. Yang, Nat. Mater. **9**, 619 (2010).
[20]F. Spaepen, Acta Metall. **25**, 407 (1977).
[21]A. S. Argon, Acta Metall. **27**, 47 (1979).
[22]M. L. Falk and J. S. Langer, Phys. Rev. E **57**, 7192 (1998).
[23]B. A. Sun, S. Pauly, J. Hu, W. H. Wang, U. Kühn, and J. Eckert, Phys. Rev. Lett. **110**, 225501 (2013).
[24]H. B. Ke, B. A. Sun, C. T. Liu, and Y. Yang, Acta Mater. **63**, 180 (2014).
[25]F. F. Wu, Z. F. Zhang, and S. X. Mao, J. Mater. Res. **22**, 501 (2007).
[26]J. Hu, B. A. Sun, Y. Yang, C. T. Liu, S. Pauly, Y. X. Weng, and J. Eckert, Intermetallics **66**, 31 (2015).
[27]J. W. Qiao, Z. Wang, Z. M. Jiao, H. J. Yang, S. G. Ma, Z. H. Wang, and B. S. Xu, Mater. Sci. Eng., A **609**, 222 (2014).
[28]Z. Wang, J. W. Qiao, G. Wang, K. A. Dahmen, P. K. Liaw, Z. H. Wang, B. C. Wang, and B. S. Xu, Mater. Sci. Eng., A **639**, 663 (2015).
[29]Y. Yang, J. C. Ye, J. Lu, P. K. Liaw, and C. T. Liu, Appl. Phys. Lett. **96**, 011905 (2010).
[30]B. A. Sun, S. Pauly, J. Tan, M. Stoica, W. H. Wang, U. Kühn, and J. Eckert, Acta Mater. **60**, 4160 (2012).
[31]G. Ananthakrishna, S. J. Noronha, C. Fressengeas, and L. P. Kubin, Phys. Rev. E **60**, 5455 (1999).
[32]Y. Estrin, K. Chihab, L. P. Kubin, and J. Vergnol, Scr. Mater. **21**, 203 (1987).
[33]G. Wang, K. C. Chan, L. Xia, P. Yu, J. Shen, and W. H. Wang, Acta Mater. **57**, 6146 (2009).
[34]P. Bak, C. Tang, and K. Wiesenfeld, Phys. Rev. A **38**, 364 (1988).